ADVANCED SUSTAINABLE SYSTEMS

Supporting Information

for *Adv. Sustainable Syst.*, DOI 10.1002/adsu.202400060

Inkjet-Printed Red-Emitting Flexible LEDs Based on Sustainable Inks of Layered Tin Iodide Perovskite

Giovanni Vescio, Dmitry N. Dirin, Sergio González-Torres, Jesús Sanchez-Diaz, Rosario Vidal, Iván P. Franco, Samrat Das Adhikari, Vladimir S. Chirvony, Juan P. Martínez-Pastor, Felipe A. Vinocour Pacheco, Lukasz Przypis, Senol Öz, Sergi Hernández, Albert Cirera, Iván Mora-Seró, Maksym V. Kovalenko and Blas Garrido*

Supplementary Materials for

Inkjet-printed red-emitting flexible LEDs based on sustainable inks of layered tin iodide perovskite

Giovanni Vescio,[1]* Dmitry N. Dirin,[2] Sergio González-Torres,[1] Jesús Sanchez-Diaz,[3] Rosario Vidal,[4] Iván P. Franco[3,4], Samrat Das Adhikari,[3] Vladimir S. Chirvony,[5] Juan P. Martínez-Pastor,[5] Felipe A. Vinocour Pacheco,[6] Lukasz Przypis,[7] Senol Öz,[8,9] Sergi Herández,[1] Albert Cirera,[1] Iván Mora-Seró,[3] Maksym V. Kovalenko,[2] Blas Garrido[1].

1) MIND-IN[2]UB, Department of Electronics and Biomedical Engineering, Universitat de Barcelona, Martí i Franquès 1, 08028 Barcelona (Spain)

2) Department of Chemistry and Applied Biosciences, ETH Zürich, Zürich CH-8093, Switzerland; Laboratory for Thin Films and Photovoltaics, Empa - Swiss Federal Laboratories for Materials Science and Technology, Dübendorf CH-8600, Switzerland

3) Institute of Advanced Materials (INAM), Universitat Jaume I (UJI), Avenida de Vicent Sos Baynat, s/n, Castelló de la Plana 12071, Spain.

4) Department of Mechanical Engineering and Construction, GID, Universitat Jaume I, Av. SosBaynat s/n, 12071 Castelló, Spain

5) UMDO, Instituto de Ciencia de los Materiales, Universidad de Valencia, Valencia 46980, Spain

6) Saule Research Institute, 54-427 Wroclaw, Poland

7) Department of Semiconductor Materials Engineering, Wroclaw University of Science and Technology, 50-370 Wroclaw, Poland;

8) Saule Technologies, 54-427 Wroclaw, Poland

9) Solaveni GmbH, 59199 Bönen, Germany

Corresponding Authors: gvescio@ub.edu

This Word document file includes:

Figures from S1 to S6

Video SV1

Tables from S1 to S5

EXPERIMENTAL PROCEDURES

Materials

Thiophene-2-ethylamine (TEA, 98 %, ABCR), hydroiodic acid (57 % with stabilizer, ABCR), diethyl ether (99.5%, Aldrich), ethanol extra dry (Acros), diisobutylaluminium hydride (DiBAl, 1M in toluene, Aldrich), borane tert-butylamine complex (97 %, ABCR), $NaBH_4$ (Aldrich), tin fluoride (99% Acros), have been used as received.

SnI_2 (99%, STREM) has been purified by sublimation in ultrahigh vacuum (10-7 mbar, 380 °C) following by washing in anhydrous acetone for 30 minutes and drying under vacuum (5 mbar) for 1 hour.

2,3,5,6-tetramethyl-1,4-bis(trimethylsilyl)-1,4-diaza-2,5-cyclohexadiene (Mashima reagent) has been kindly provided by Prof. Christophe Copéret (ETH Zurich).

2,4,6-tris[3-(diphenylphosphinyl)phenyl]-1,3,5-triazine (PO-T2T) was purchased from Lumtec Taiwan. PEDOT:PSS Al 4083 aqueous solution was purchased from Heraeus. Phenylethylammonium iodide (PEAI. 98%) was purchased from Greatcell solar materials. All materials were use as received with no further purifications. Prepatterned ITO glass substrates (6 pixels) were purchased from Ossila. prepatterned ITO flexible polyimide substrates (4 pixels) were purchased from Biotain.

Ink preparation

TEA_2SnI_4 precursor solution has been prepared by dissolving pre-synthesized TEAI and purified SnI_2 with 2:1 molar ratio in DMSO or DMF, overall following [10.1021/acs.jpclett.9b03565].
For the synthesis of TEAI, equimolar 2-thiopheneethyllamine (TEA, 5.190 g, 4.8 ml, 40.8 mmol) and hydroiodic acid (HI, 9.18 g, 5.4 ml, 40.8 mmol) were dissolved in ethanol (10 ml for each), mixed, and stirred for 1 hours in an ice bath. After the reaction, the solvent was rotary evaporated. After that, the TEAI was redissolved in ethanol and precipitated with diethyl ether. The obtained white crystals were vacuum-dried at room temperature for 72 h and stored inside the glovebox.
Purification of SnI_2. We have found that available commercial sources of SnI_2 (Alfa and Strem) are heavily contaminated. All suppliers guarantee >99% metal basis purity. However, all tested batches of SnI_2 contained other Sn-based impurities, such as SnO, SnO_2 and SnI_4. Although the first two impurities might not be crucial in non-hot-injection synthesis, the latter may change optical properties of the synthesized TEA_2SnI_4 significantly as it can create deep trap states within the bandgap. Therefore, we have used the purification procedure developed earlier for the synthesis of $FASnI_3$ NCs. We have purified commercial SnI_2 by sublimation in ultrahigh vacuum (10^{-7} mbar, 380 °C) following by washing in anhydrous toluene for 30 minutes and drying under vacuum (5 mbar) for 1 hour.

Inkjet printing and thermal treatments of TEA_2SnI_4 layer

The details of the printing procedure of the TEA_2SnI_4 are indicated as follows: the ink formulation was based on pure DMF or DMSO solvents. An ink ejection frequency of 2.0 kHz (for DMF-based) and 0.9 kHz (DMSO-based) and a resolution of 630 drops per inch (DPI) was used. During the TEA_2SnI_4 layer printing, the platen substrate temperature was kept constant below 20 °C in order to promote a proper spreading and adhesion among the different sublayers piled up to complete the thick full layer. After the inkjet-printing process, the layers were submitted to the curing

process based on vacuum annealing at 85 °C 10 minutes (DMF-based solution) and 110 °C for 10 minutes (DMSO-based solution).

Device Fabrication

The PEDOT:PSS solution was filtered with 0.45 μm PVDF filter and spin coated on top of ITO at 5,000 rpm (2,000 rpm/s of acceleration) for 40 s and annealed at 130 °C for 20 min in ambient conditions. After the hole transporting layer (HTL) deposition the substrates were introduced in a N_2-filled glovebox, for the TEA_2SnI_4 inkjet printing layer deposition. The filtered solution of perovskite ink, with a viscosity around ~2 cP, was printed with a fixed drop-volume of 10 pL through 21-μm diameter nozzle by using cartridge for Dimatix printers (Fujifilm Dimatix Inc.) on top of PEDOT:PSS-coated layers. The preparation of the inks and the printing processes were both carried out in a glove box.

Finally, the substrates were transferred to a vacuum chamber, to evaporate 40 nm of PO-T2T, 1 nm of LiF and 100 nm of Al. The area of the flexible device was defined by the evaporation mask, which was 0.08 cm^2.

Inkjet-printed film/device characterization

The morphology and structure of Inkjet-printed perovskite thin films were studied by field emission scanning electron microscope (FEGSEM - JEOL 3100F) operated at 15 kV.

The crystalline microstructure, orientation and size of the NCs were determined by XRD using a Japan Rigaku D/Max-IIA X-ray diffractometer using Cu Kα radiation, l = 1.5406 Å, operating at 40 keV and 40 mA.

The optical properties were evaluated by measuring the transmittance and reflectance spectra, by using an integrating sphere (Bentham PV300 EQE system), using monochromated light from a Xe and quartz halogen dual lamp source through the 300–1100 nm range, and collecting the transmitted (or reflected) light with an InGaAs photodetector. Finally, the emission properties were determined by acquiring photoluminescence (PL) spectra of the films grown onto Si substrates, exciting the samples with the 325-nm line of a He-Cd laser, with a power density of 8×10^3 W cm^{-2}, and analyzing the emitted light with a single-grating monochromator coupled to a GaAs photomultiplier.

External quantal efficiency (EQE) measurements were performed with a QEPVSI-b Oriel system. Stability measurements were performed fixing the voltage.

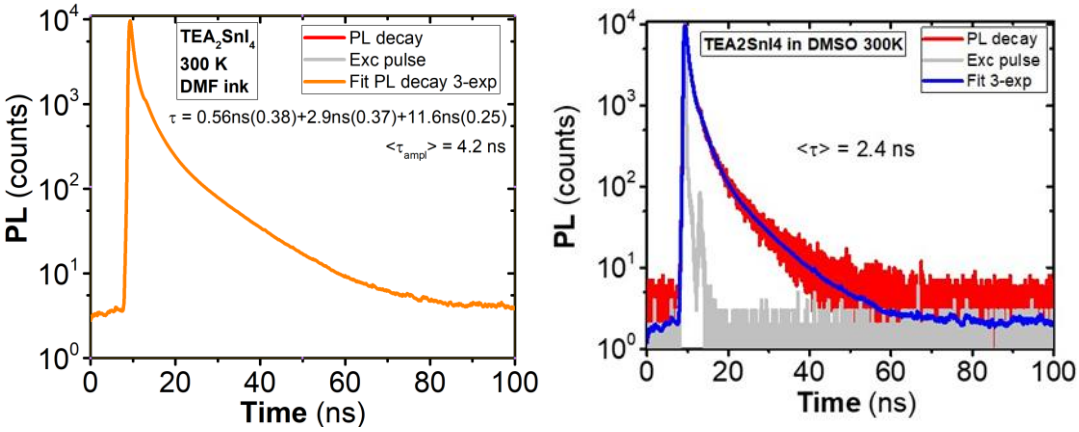

Figure S1 : Room temperature PL properties of TEA_2SnI_4 films inkjet-printed on a flexible polyimide substrate: PL decay kinetics of the films deposited by using DMF and DMSO based ink and results of its 3-exponential fitting with τ_1 = 0.56 ns (38%), τ_2 = 2.9 ns (37%), τ_3 = 11.6 ns (25%) and average PL lifetime of 4.2 ns;

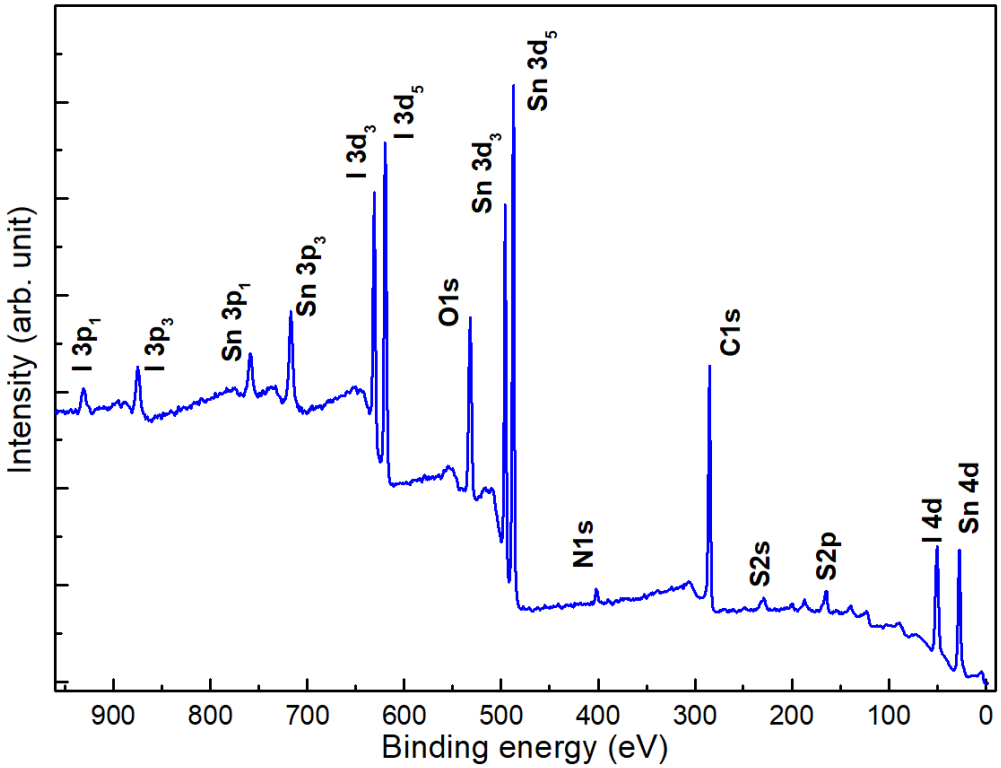

Figure S2: XPS binding energy survey for both tested inks.

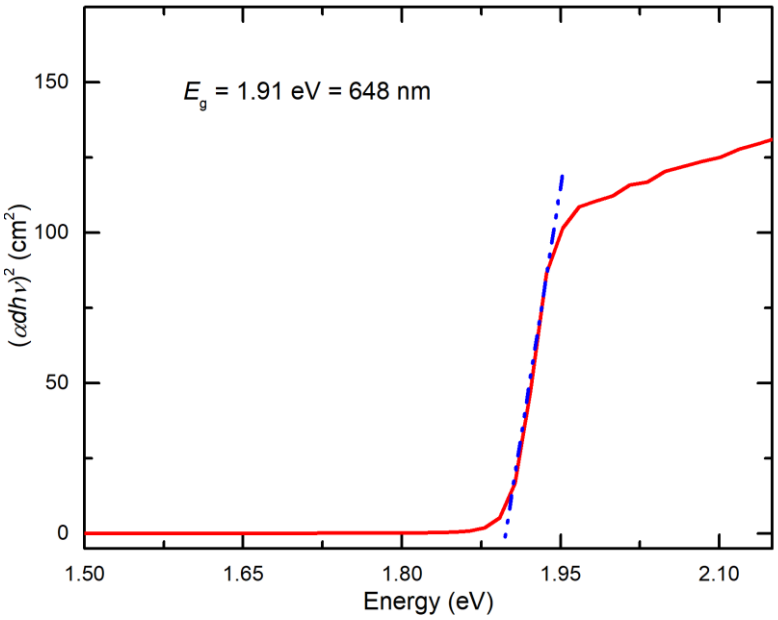

Figure S3: Tauc plot of inkjet-printed TEA_2SnI_4 after subtracting the excitonic emission.

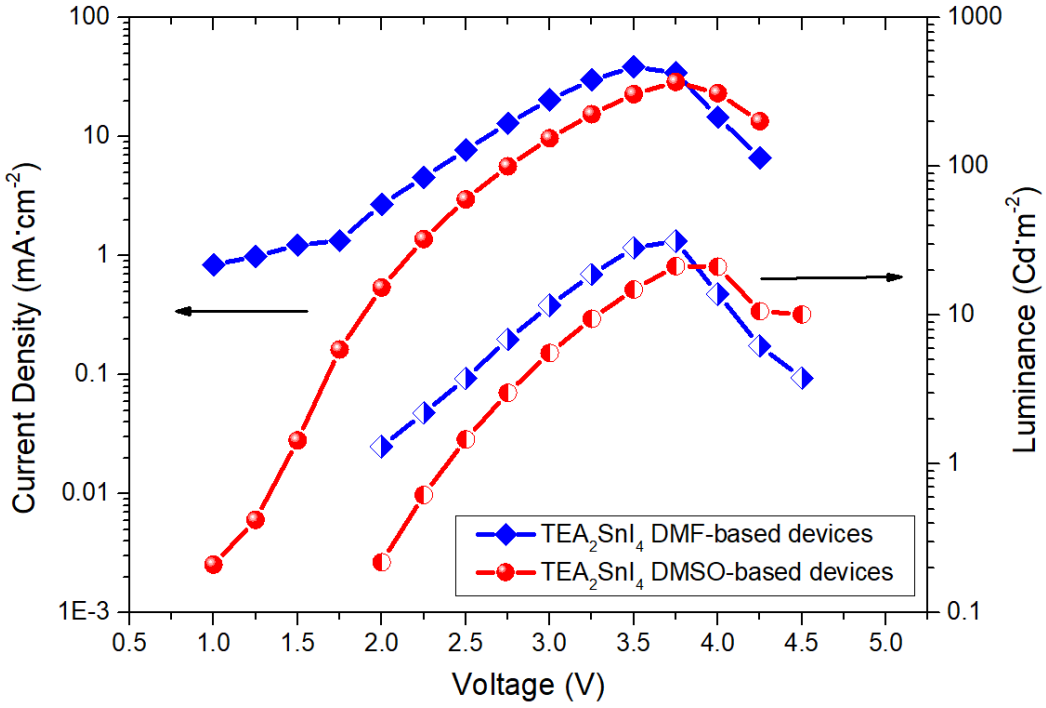

Figure S4: Current density and luminance vs voltage characteristics on glass substrate. The results for LEDs with inkjet printed TEA_2SnI_4 film prepared with DMF-based and with DMSO-based solvents.

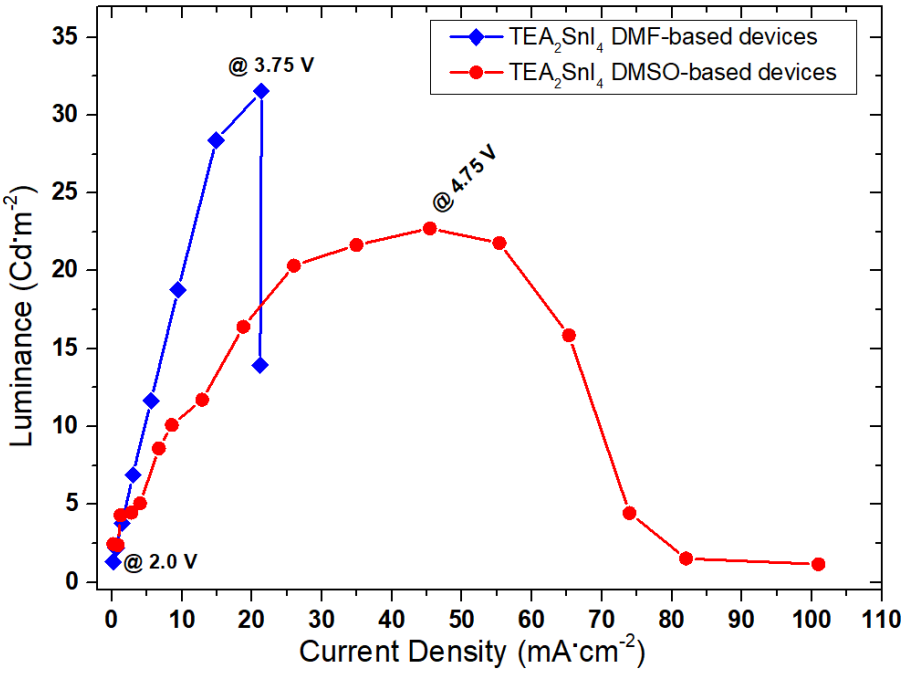

Figure S5: Luminance versus current density characteristics on flexible substrate.

Figure SV1: Video of an array of 6 pixels LED red emitting based on 2D perovskite TEA_2SnI_4 under 5 V voltage applied.

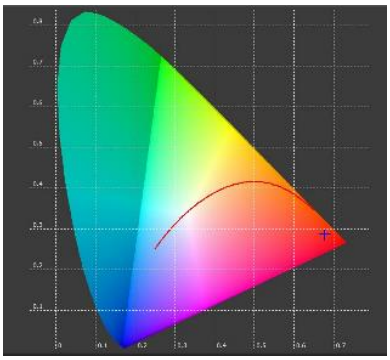

Figure S6: *EQE versus voltage characteristics; b) Color coordinate in the CIE 1931 chromaticity diagram of the EL spectra.*

Comparative life cycle assessment of perovskite inks

Life cycle inventories considered for comparing the two printed inks are associated with the quantity and type of solvent required for the perovskite solution, electricity consumption during printing and annealing, air emissions of solvents during drying, and the differential wear of cartridges and printheads. Differences in experimental procedure for perovskite layer deposition with DMF and DMSO are explained in section "**Inkjet printing and thermal treatments of TEA_2SnI_4 layer**" of this supplementary info. The values are detailed in Table S1 and expounded upon below.

Table S1: Comparative inventories for 1 cm^2 of inkjet printed TEA_2SnI_4 film prepared with DMF-based and with DMSO-based solvents

	Flow	Unit	DMF	DMSO
Input	Solvent production	kg	3.45E-04	$4.02\ 10^{-4}$
	Electricity	MJ	1.98E-02	$2.80\ 10^{-2}$
	Cartridge	p	4.58E-03	$8.22\ 10^{-5}$
Output	Solvent emission	kg	3.45E-04	$4.02\ 10^{-4}$
	Cartridge	p	4.58E-03	$8.22\ 10^{-5}$

The Life Cycle Assessment (LCA) of solvents for perovskite layer deposition, encompassing production and emissions, has been previously documented for DMF and DMSO.[3] Novel human toxicity characterization factors were derived by applying fate and exposure models utilizing available data from the European Chemicals Agency (ECHA), with which USEtox[4] was updated.

Electricity consumption was measured in equipment owned by the Universitat de Barcelona, utilizing the CIRCUTOR AR5 electrical analyzer with a sampling rate of 2 kHz and recording every second for a 4 cm^2 surface. Printing is executed with the inkjet printer FUJIFILM Dimatix DMP-2831 alongside a computer. DMOS inks are printed at 0.9 - 1 kHz, and DMF at 2 kHz. Annealing is performed using a PELCO 2245 mini hot-vacuum chamber coupled with a hot plate Onilab MS-H-Pro for 10 minutes at 85°C for DMF and 110°C for DMSO. Electricity consumptions are presented in Table S2.

Table S2: Energy consumption for inkjet printed TEA_2SnI_4 film prepared with DMF-based and with DMSO-based solvents.

Solvent	Process	Power (W)	Time (s)	Energy (kWh)
DMF	Inkjet printer	87.04	132.5	$3.20\ 10^{-3}$
	Computer	61.18	132.5	$2.25\ 10^{-3}$
	Mini Hot Vacuum	28.10	600.0	$3.27\ 10^{-5}$
DMSO	Inkjet printer	85.71	189.5	$4.51\ 10^{-3}$
	Computer	60.72	189.5	$3.20\ 10^{-3}$
	Mini Hot Vacuum	58.72	600.0	$6.84\ 10^{-5}$

Environmental impacts resulting from energy consumption in the inkjet printing process were calculated using the Spanish electricity mix for 2020,[5] based on primary energy from the Eurostat database (nrg_ind_pehcf), pass-through coefficients for Europe provided by JEC WTT,[6] energy flows from Ecoinvent 3.6 database and energy transmission and distribution losses.[7] Electricity flows were modeled with SimaPro software, considering a 1.9% loss in high voltage lines and a 7.1% loss in medium voltage lines.

Cartridges are used continuously for one working day with DMF as a solvent and then discarded. Cartridges used for inks with DMSO are refilled over an average of 4 months. Disposal and recycling of cartridges and printheads follow the methodology and datasets provided by the WEEE LCI project.[8] Inventories for the manufacturing of cartridges and printheads were obtained by weighing different assemblies and identifying them with the support of patents and literature.[9,10] Inventories from cradle to gate and for end-of-life (EOL) are detailed in Table S3 and Table S4, respectively.

Table S3: Cradle to gate inventory for one cartridge and printhead for Inkjet printer FUJIFILM Dimatix.

Part	Flow	Unit	Quantity	Observations
Case Cartridge	PP	g	16.970	Polypropylene, granulate {RoW}+ Injection moulding {RoW}
Case Printhead	ABS	g	10.947	Acrylonitrile-butadiene-styrene copolymer {RoW} + Injection moulding {RoW}
Thermistors	Cu	g	0.042	Copper {RoW} + Sheet rolling, copper {RoW}
Resistor	Al_2O_3	g	0.042	Aluminium oxide, non-metallurgical {RoW} + Resistor, auxilliaries and energy use {GLO}
Flexible printed circuit	PMMA+Cu	g	0.128	Printed wiring board, for surface mounting, Pb free surface {GLO} without GFRP + Polymethyl methacrylate, sheet {RoW}. 35 µm of Cu and 75 µm of polymer.
Ink channel	ABS	g	0.289	Acrylonitrile-butadiene-styrene copolymer {RoW} + Injection moulding {RoW}
Pumping chamber	Al_2O_3	g	0.413	Aluminium oxide, non-metallurgical {RoW} + Resistor, auxilliaries and energy use {GLO}
Transport	Transport freight sea	kgkm	187.557	Transport, freight, sea, container ship {GLO}. From Boston port to Barcelona port
Transport	Transport road	kgkm	6.430	Transport, freight, lorry, unspecified {RoW}

Table S4: *End of life for one cartridge and printhead for Inkjet printer FUJIFILM Dimatix. Datasets provided by WEEE LCI project.*[10]

Part	Flow	Unit	Quantity	Observations
Cartridge	PP	g	16.973	EoL, Small Professional Elec. Equip. PP without BFR, density < 1.3, Substitution benefits not included
Printhead	ABS	g	11.861	EoL, Small Professional Elec. Equip. ABS without BFR, density < 1.3, Substitution benefits not included

The impact assessment was conducted using the ReCiPe 2016 v1.04 method incorporated within the LCA software SimaPro 9.4. ReCiPe2016 provides a state-of-the-art impact assessment method, converting Life Cycle Inventory (LCI) into harmonized impact scores at midpoint and endpoint levels.[12] The study follows a hierarchist perspective based on scientific consensus regarding time horizon, adaptation capacity and technology development. Inventories from the Ecoinvent database were allocated according to the cut-off system model.[13]

Environmental impact categories considered fall under the human health area of protection: human toxicity, global warming, particulate matter, and other impacts (stratospheric ozone depletion, ionizing radiations, ozone formation, and water consumption). The common unit used is DALY. Environmental impacts, calculated with the ReCiPE Midpoint method, are also detailed: global warming, stratospheric ozone depletion, ozone formation over human health, and fine particulate matter formation. At the midpoint level, impact categories are not grouped into areas of protection. Selected midpoint impact categories and endpoint impact categories for human health are summarized in Table S5.

Table S5: Environmental impact evaluation for inkjet printed TEA_2SnI_4 film prepared with DMF-based and with DMSO-based solvents. Environmental aspects included are solvent production, solvent emission during perovskite deposition, electricity consumption for inkjet printing and annealing, and cartridge manufacturing and disposal. The functional unit is 1 cm^2 of printed perovskite.

	Category		Unit	DMF	DMSO
Endpoint	Environment Human Health	HH	DALY	$8.91\ 10^{-9}$	$5.46\ 10^{-9}$
	Human health toxicity	HHT	DALY	$3.19\ 10^{-9}$	$1.29\ 10^{-9}$
	Global warming	GW	DALY	$2.89\ 10^{-9}$	$2.23\ 10^{-9}$
	Particulate matter	PM	DALY	$2.51\ 10^{-9}$	$1.53\ 10^{-9}$
	Others	Others	DALY	$3.27\ 10^{-10}$	$4.23\ 10^{-10}$
Midpoint	Global warming	GW	kg $CO_{2\ eq}$	$3.11\ 10^{-3}$	$2.39\ 10^{-3}$
	Stratospheric ozone depletion	OD	kg $CFC_{11\ eq}$	$1.70\ 10^{-9}$	$1.66\ 10^{-9}$
	Ionizing radiation	IR	kBq $Co_{-60\ eq}$	$1.04\ 10^{-3}$	$1.37\ 10^{-3}$
	Ozone formation, Human health	OF	kg $NO_{x\ eq}$	$6.17\ 10^{-6}$	$4.53\ 10^{-6}$
	Fine particulate matter formation	PM	kg $PM_{2.5\ eq}$	$3.99\ 10^{-6}$	$2.41\ 10^{-6}$

References

[1] Z. Wang, F. Wang, B. Zhao, S. Qu, T. Hayat, A. Alsaedi, L. Sui, K. Yuan, J. Zhang, Z. Wei, Z. Tan, *Journal of Physical Chemistry Letters* **2020**, *11*, 1120.

[2] G. Vescio, J. Sánchez-Diaz, J. L. Frieiro, R. Sánchez, S. Hernández, A. Cirera, I. Mora-Seró, B. Garrido, *ACS Energy Lett* **n.d.**, *7*, 3653.

3. Vidal, R. et al. Assessing health and environmental impacts of solvents for producing perovskite solar cells. Nat. Sustain. (2020). doi:10.1038/s41893-020-00645-8

4. Rosenbaum, R. K. et al. USEtox human exposure and toxicity factors for comparative assessment of toxic emissions in life cycle analysis: Sensitivity to key chemical properties. Int. J. Life Cycle Assess. 16, 710–727 (2011).

5. Red Electrica de España. El Sistema Eléctrico Español 2020. Red Eléctrica de España (REE). (2021).

6. Prussi, M. et al. JEC Well-to-Tank report v5. (2020). doi:10.2760/959137

7. CNMC. Boletines de indicadores eléctricos. Available at: https://www.cnmc.es/listado/sucesos_energia_mercado_electrico_boletines_de_indicadores_electricos/block/250.

8. Bleu Safran. End-of-life management LCI of constituent materials of Electrical and Electronic Equipment (EEE) within the framework of the French WEEE take-back scheme Methodological summary. (2018).

9. Bibls, A., Higginson, J. A., Von Essen, K. & Xu, A. Single-use droplet ejection module. (2006).

10. Muguruza Blanco, A. Contribución a las tecnologías de fabricación aditiva para la obtención de piezas multimaterial, combinando la impresión 3D por máscara con la impresión funcional mediante sistemas InkJet. (Universitat Politècnica de Catalunya Barcelona, 2019).

11. Bleu Safran, *End-of-Life Management LCI of Constituent Materials of Electrical and Electronic Equipment (EEE) within the Framework of the French WEEE Take-Back Scheme Methodological Summary*, **2018**.

12. Huijbregts, M. A. J. et al. ReCiPe2016: a harmonised life cycle impact assessment method at midpoint and endpoint level. Int. J. Life Cycle Assess. 22, 138–147 (2017).

13. Ecoinvent Centre. Cut-Off System Model. Ecoinvent Online (2018). Available at: https://www.ecoinvent.org/database/system-models-in-ecoinvent-3/cut-off-system-model/allocation-cut-off-by-classification.html. (Accessed: 7th August 2020